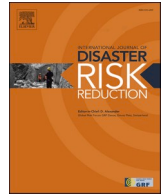


Contents lists available at [ScienceDirect](https://www.sciencedirect.com)

## International Journal of Disaster Risk Reduction

journal homepage: [www.elsevier.com/locate/ijdrr](http://www.elsevier.com/locate/ijdrr)

# Impact of future tsunamis from the Java trench on household welfare: Merging geophysics and economics through catastrophe modelling

Dimitra M. Salmanidou<sup>a,\*</sup>, Ayao Ehara<sup>a</sup>, Rozana Himaz<sup>b</sup>, Mohammad Heidarzadeh<sup>c</sup>, Serge Guillas<sup>a</sup>

<sup>a</sup> Department of Statistical Science, University College London, United Kingdom

<sup>b</sup> Business School, Oxford Brookes University, United Kingdom

<sup>c</sup> Department of Civil and Environmental Engineering, Brunel University London, Uxbridge, UB8 3PH, United Kingdom

## ARTICLE INFO

## Keywords:

Natural disasters  
Risk modelling  
Insurance  
Vulnerability  
Disaster risk finance  
Indonesia

## ABSTRACT

This paper presents the first end-to-end example of a risk model for loss of assets in households due to possible future tsunamis. There is a significant need for Government to assess the generic risk to buildings, and the concrete impact on the full range of assets of households, including the ones that are key to livelihoods such as agricultural land, fishing boats, livestock and equipment. Our approach relies on the Oasis Loss Modelling Framework to integrate hazard and risk. We first generate 25 representative events of tsunamigenic earthquakes off the Southern coast of Java, Indonesia. We then create a new vulnerability function based upon the Indonesian household survey STAR1 of how much assets have been reduced in each household after the 2004 tsunami. We run a multinomial logit regression to precisely allocate the probabilistic impacts to bins that correspond with levels of financial reduction in assets. We focus on the town of Cilacap for which we build loss exceedance curves, which represent the financial losses that may be exceeded at a range of future timelines, using future tsunami inundations over a surveyed layout and value of assets over the city. Our loss calculations show that losses increase sharply, especially for events with return periods beyond 250 years. These series of computations will allow more accurate investigations of impacts on livelihoods and thus will help design mitigation strategies as well as policies to minimize suffering from tsunamis.

## 1. Introduction

Tsunamis are major worldwide disasters; large events in 2004 and 2011 have reached death counts of approximately 228,000 and 18,000, and many more injuries, across the Indian Ocean and Japan [1]. Smaller events that are less widespread may still have a huge effect on local communities. One aspect that has been overlooked is the impact that such catastrophes have had, and will have, on livelihoods, due to a lack of methods to quantify these consequences. Since communities can be severely affected by the loss of their essential means of survival, the academic community needs to provide such approaches and aid policy-makers to design policies that can mitigate future events. However, these challenges are sizeable since this research requires the involvement of multiple disciplines: Earth Sciences, Numerical Modelling, Statistics, and Economics. In this paper a first proof-of-concept illustration is provided, for a small region of Indonesia, of how these

research fields can be combined to provide estimates of future impacts of tsunamis originating south of Java, on livelihoods and household welfare.

Indonesia is among the most active tsunamigenic regions in the world and was the site of two destructive tsunamis in the past few years in Sulawesi (September 2018) [2,3] and in Sunda Strait (December 2018) [4,5]. The aforesaid tsunamis caused 4,340 [6] and 437 [7] deaths, respectively, as well as significant damage<sup>1</sup>. The tsunami catalogue by Hamzah et al. [8] identified 105 tsunamis in Indonesia in the period 1600-1999 AD occurring in six main tsunamigenic zones. Prasetya et al. [9] reported 18 tsunamis in Indonesia since 1900 AD. It was shown that 90% of past tsunamis in Indonesia were generated by earthquakes [8], highlighting the importance of understanding these types of tsunamis in the country. Among Indonesia's six tsunamigenic zones [8] is the Eastern Sunda Arc zone spanning from Sunda Strait, in northwest, to Flores Island, in southeast (Fig. 1). This region is a

\* Corresponding author.

E-mail address: [d.salmanidou.12@ucl.ac.uk](mailto:d.salmanidou.12@ucl.ac.uk) (D.M. Salmanidou).

<sup>1</sup> The terms damage and loss are used interchangeably in the text.

<https://doi.org/10.1016/j.ijdrr.2021.102291>

Received 11 August 2020; Received in revised form 21 April 2021; Accepted 26 April 2021

Available online 14 May 2021

2212-4209/© 2021 The Author(s).

Published by Elsevier Ltd.

This is an open access article under the CC BY-NC-ND license

(<http://creativecommons.org/licenses/by-nc-nd/4.0/>).

seismic-active zone with approximately 50 Mw > 6.5 earthquakes in the past 100 years according to the US Geological Survey (USGS) catalogue<sup>2</sup>. The seismic activity here is due to the presence of the Java trench (Fig. 1) which is the result of northeast subduction of the Indo-Australian Plate beneath the Sunda Plate.

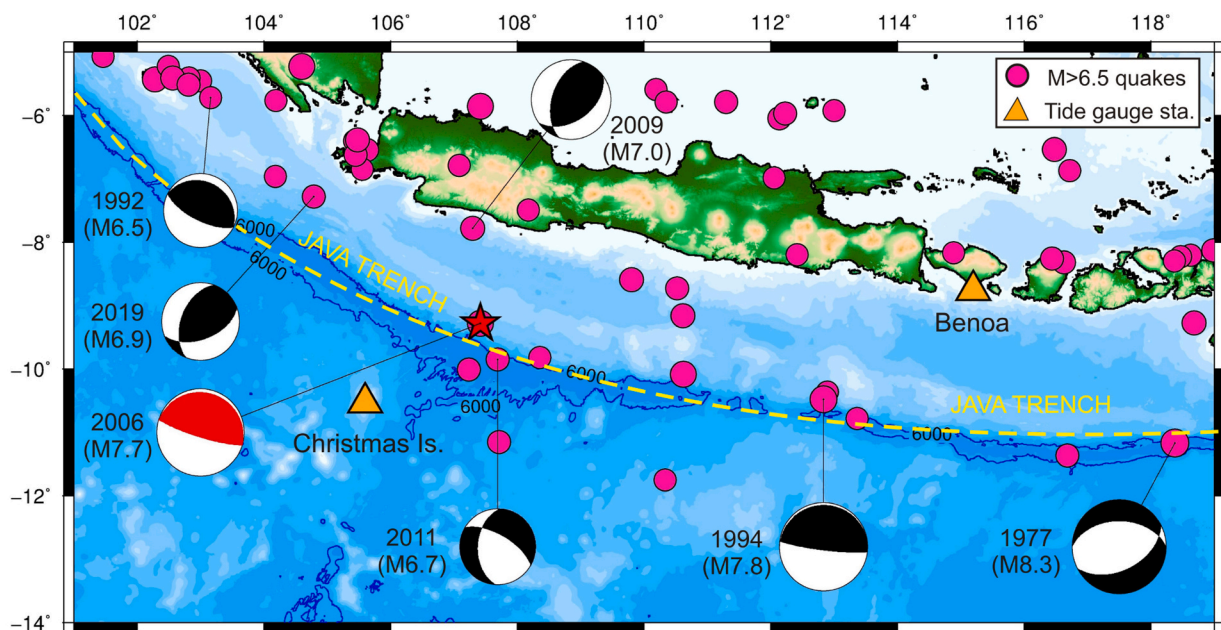
The Java trench in central Indonesia has given rise to numerous tsunamis in the past [8]. One of the most recent catastrophic events affecting the region was the 2006 earthquake and tsunami. The so-called Pangandaran earthquake (after the worst hit region) occurred on July 17, 2006 and registered a moment magnitude of Mw 7.7, circa 200 km south of Java (International Tsunami Information Center- ITIC<sup>3</sup>). The slow rupture gave rise to a tsunami that hit the coastlines of Java with little time for early warning due to the small amount of felt ground shaking and the source proximity to the shore [10]. More than 800 people perished and over 300 km of coastline was affected by the event [10,11]. Tsunami waveforms of the 2006 event, recorded by a few tide gauges, are shown in Fig. 1. Another large tsunamigenic earthquake (Mw 7.8) in this region occurred on June 3, 1994 resulting in a tsunami that killed over 200 people [12]. Both 1994 and 2006 events were characterised as tsunami earthquakes [12,13]: events that rise to larger tsunamis than expected from their moment magnitudes [14]. Other historical events that affected the region span across the last century

(1921, 1937, 1943 and 1977) [15,16]. The largest of them was the 1977 outer-rise earthquake with Mw 8.3 (Fig. 1). The tsunami recorded maximum run-up height of 5.8 m and maximum inundation distance of 1.2 km on Sumba island [15].

Risk modelling for tsunamis has so far mostly focused on buildings. These assets have been of primary interest to the (re-)insurance industry, the largest user of loss modelling platforms such as the Oasis Loss Modelling Framework. However, a small percentage of Indonesian households and small businesses are insured against losses from direct damages to buildings. There is also limited access to business interruption that covers the wider range of assets that they possess to sustain themselves (e.g. agricultural land and livestock, fishing boats and nets, etc). Furthermore, insurance penetration and density rates are very low compared to other Asian countries and the World [17,18]. This results in a mismatch between what modelling platforms can compute and what actual losses would ensue from a tsunami (or another disaster).

The aim of this research is to present a proof-of-concept study that can be extended to wider ranges of tsunami variations, over larger regions and even extend to other types of tsunamis (generated by landslides, volcanic activity and others), as well as to other types of hazards. The objective of this research is to provide for the first time an end-to-end modelling by using damage to household level business and non-

**a) Seismicity of Java subduction zone**



**b) Waveforms of July 2006 tsunami**

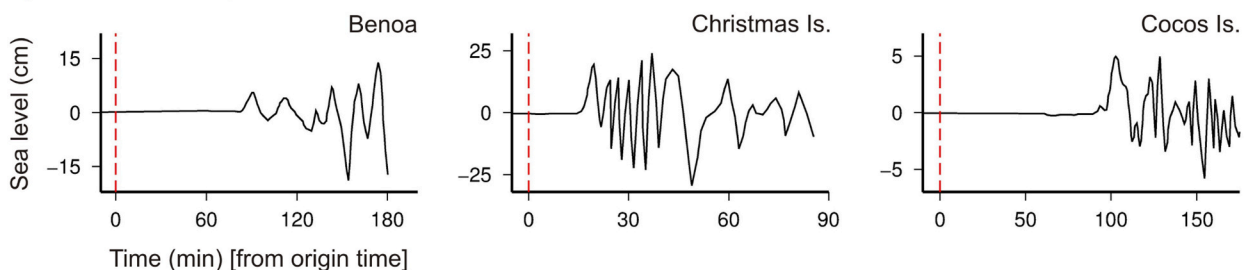


**Fig. 1.** a) Area of interest and focal mechanisms of past earthquake events in the Java trench, b) Tide gauge records of the 2006 tsunami.

<sup>2</sup> <https://earthquake.usgs.gov/earthquakes/search/>.

<sup>3</sup> <http://itic.ioc-unesco.org/index.php>.

business assets as a proxy for impacts on household welfare.

The questions are multiple in order to quantify the tsunami impacts: What hazard intensities will trigger impacts and by how much? Where

are the exposed assets? What monetary value have these assets locally? How impacts on household welfare based on historical events help estimate damages from future tsunamis? What are the event distributions of future tsunamis and how to weigh low probability-high impact ones vs. more frequent but less damaging ones? How to integrate these computations into a loss modelling platform that allows for probabilistic computations to be carried out? The answers provided below focus on the livelihood aspect. We suggest a simplified setting for the tsunamis (25 representative events that we repeat with weights corresponding to expected frequencies), over a small region (the city of Cilacap in Java).

## 2. Simulations of tsunami hazard

### 2.1. Experimental set-up

Tsunami hazard assessment is usually carried out by probabilistic approaches. Here, we adapt a simple pseudo-probabilistic approach to study tsunami hazards along the Indonesian coast of Java since our aim is to demonstrate the potential for realistic future welfare impact studies using a fully probabilistic approach over the entire coastline. An enhanced probabilistically generated set of scenarios will further improve, but may not radically modify these findings. We study maximum run-up height and inundation distance under a range of large to great earthquakes in the Java trench. We quantify the potential impacts of such tsunamigenic earthquakes from the Java subduction zone on the coastal areas. A tsunami numerical model is adopted for the region, and is validated benefiting from the observation data of the 2006 Java earthquake and tsunami as reported by Fujii and Satake [11]. We then model tsunami generation induced by 25 earthquakes with moment magnitudes in the range of 7.9–9.0. We numerically calculate the coastal run-up of these events and focus our simulations on tsunami inundation in populated areas that were affected during earlier tsunami events (e.g. the 2006 Java tsunami).

To simulate the tsunami events, we make use of the numerical code JAGURS [19–21]. The code solves the nonlinear shallow water and the Boussinesq equations and has been efficiently used to model earthquake [19,20] and landslide tsunamis [22,23] in the past. In our study we make use of the nonlinear shallow water equations, the computation of the crustal displacement is integrated in the code following the Okada dislocation model [24]. One grid is used in the modelling of the 2006 event with longitudes of 96°E–119°E and latitudes of 05°S–14°S and with a spatial resolution of  $\Delta x = \Delta y = 0.004^\circ$ . The bathymetry and elevation data derived from the General Bathymetric Chart of the Oceans (GEBCO) as a part of the GEBCO\_2019 Grid product that has a resolution of 15 arc-seconds.

The utilisation of nested grids allows us to focus in the areas of interest to study the impact of large earthquake scenarios. In total we use 3 nested grids spanning across 3 different resolution layers with a grid ratio of 1 : 4. The first resolution layer is the background grid SD01 which has the same properties as the grid in the simulation of the 2006 event (SD01, Fig. 2). The intermediary grid (SD02, Fig. 2) has geographical domain of 107.02°E–112.48°E in longitude and 07.02°S–08.98°S in latitude with a spatial resolution of  $\Delta x = \Delta y = 0.001^\circ$ . The third grid layer focuses on selected areas of the coastline and covers the geographical domain shown in Fig. 2, SD03 (which includes the area of Cilacap): [108.52°E–109.28°E, 07.62°S–07.80°S], with a spatial resolution of  $\Delta x = \Delta y = 0.0025^\circ$ .

The bathymetry and elevation data are derived from a compilation of sources as the GEBCO\_2019 Grid (SD01) and the Geospatial Information Agency of Indonesia (SD02–03). For the grids SD02–03, the bathymetry data originate from the National Bathymetric dataset (BATNAS) and are provided at a resolution of 6 arc-seconds while the digital elevation dataset (DEMNAS) has a spatial resolution of 0.27 arc-seconds. The data are merged into uniform grids; we treat the issue of void data that occur due to the merging with linear interpolation between the datasets, preserving the DEMNAS data for the elevation.

### 2.2. Simulation of the 2006 event

To simulate the 2006 event we take as initial source the fault parameters as estimated by Fujii and Satake [11]. The fault model assumes an instantaneous rupture across 10 sub-faults. Following Fujii and Satake [11], the slip varies from 0 m to 2.47 m with the largest slip identified in the eastern part of the fault plane. The rupture length is 200 km with each sub-fault occupying a size of 50 km × 50 km. The fault depth varies between 3 km and 11.7 km for the shallow and deep sub-faults, respectively. The focal mechanism is: dip angle = 10°, rake angle = 95° and strike angle = 289°.

We validate our numerical modelling practice using the data from the 2006 Java earthquake and tsunami. Our data include three real tide gauge records of the 2006 Java tsunami which are digitized from Fujii and Satake [11]. The locations of the gauge stations that recorded the tsunami were in the vicinity of Christmas island, Cocos islands and Benoa, the locations are shown in Fig. 3d. The comparison shows an overall agreement in the tsunami phase between the tide gauge records and the simulations (Fig. 3). Some differences in tsunami amplitudes are observed especially at the location of the Christmas gauge (Fig. 3). These could be attributed to discrepancies between the computational grid and the actual bathymetric features of the region, as the resolution of the data (GEBCO) is not high enough to capture nearshore wave characteristics. Other sources of uncertainties are the location of tide gauges (as provided by varying sources), differences in the source models and subsequently in the wave characteristics [11,25,26] and wave amplification at certain locations caused by potential secondary events such as earthquake-triggered landslides [10].

The sampling intervals of the tide gauge observations were relatively large (usually more than 1 min) which does not allow a full registration of the tsunami; therefore, lack of a perfect match between observations and simulations does not necessarily imply problems in modeling. We note that the quality of our simulation and its agreement with observation is similar to that of the original author of the source models, i.e. Fujii and Satake [11]. Here, we are not proposing a new source model for the 2006 Java earthquake, but are using a source model previously proposed by Fujii and Satake [11]; therefore, we do not perform Root Mean Square Error (RMSE) or other type of analyses as they are beyond the scope of this work.

### 2.3. Large earthquake scenarios in the Java trench

Given the lack of Mw 9 thrust events in the instrumentation data for the Java trench region, a rising question is whether the Java trench can accommodate mega-thrust events. According to McCaffrey [27] and Okal [16], any long and continuous subduction zone has the potential for great earthquakes (e.g. Mw 9) with large recurrence intervals (500 years or longer). The lack of Mw 9 earthquakes in the Java trench does not necessarily mean such events never occurred; absence of evidence can possibly be attributed to the short span of historical and instrumental data [27–30]. Paleo-tsunami and historical archival researches in other world's subduction zones has found evidence for Mw 9 events in geological layers and historical data that can be dated ~ 1,000 years ago (e.g. Refs. [31,32]). The data of our 25 tsunamigenic earthquake scenarios are shown within the Appendix, in Table 7 and include the longitudinal and latitudinal coordinates, the rupture length, depth and slip of each event. The table also presents the maximum uplift and subsidence for each scenario and the calculations of seismic moment ( $M_0$ ) and moment magnitude (Mw); for example, one of the largest earthquake scenarios, scenario 15 (Mw 9.0), has maximum uplift and subsidence of 6.4 m and –4.4 m, respectively.

To produce these 25 scenarios, we follow a pseudo-probabilistic approach which is a median approach between typical deterministic [4,30] and probabilistic [33,34] approaches. By considering minimum (Mw 7.9) and maximum (Mw 9.0) values for potential tsunamigenic earthquakes in the region, we produced 25 earthquake scenarios which

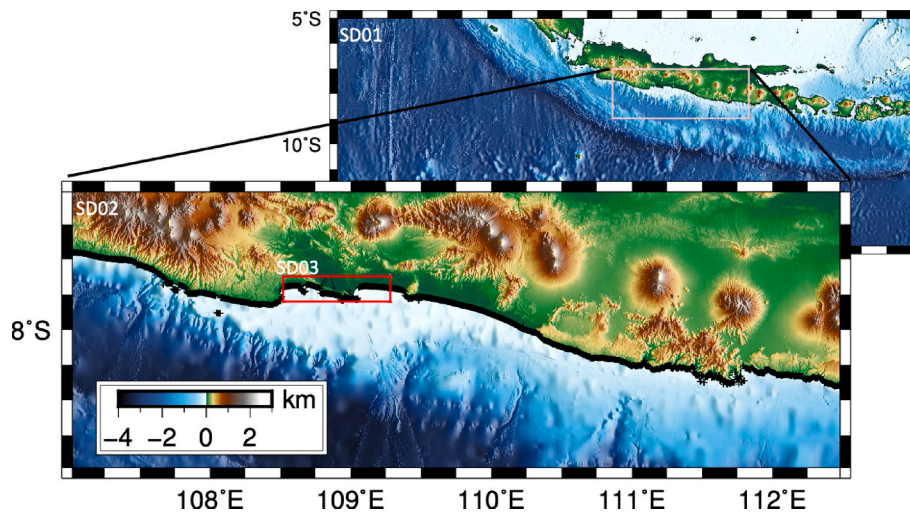


Fig. 2. The spatial domains of the simulations. The computational grid SD01 is represented in the top-right corner, the boundaries of SD02 are represented by pink color. SD02 grid ire shown in bottom-left corner, the boundaries of grids SD03 are also depicted with red colour. The black crosses (forming a dense black line) show the locations (ca. 5,400) of the shoreline from which the tsunami elevation was sampled, extracted at each coastal grid cell of SD02 (Fig. 6).

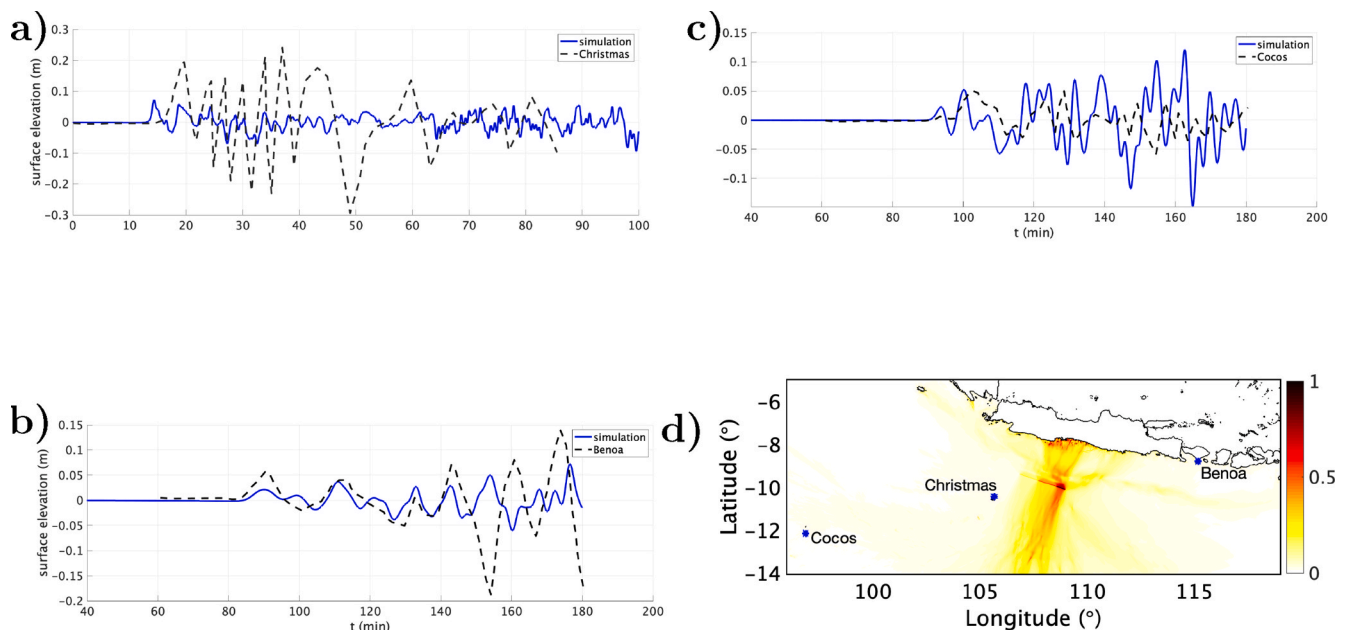


Fig. 3. Numerical results plotted against observations of the 2006 event. Panel d) represents the maximum free surface elevation from the fault displacement inferred by Fujii and Satake [11].

are distributed all along the Java Trench (Fig. 4). We took into account the geometrical and geophysical parameters of the subduction zone in our scenarios. For instance, all scenarios follow the strike angle of the subduction zone; the farther the scenarios from the trench, the deeper the depth of the earthquake becomes; the slip values are related to the length/width of the scenario earthquakes using the empirical equations of Wells and Coppersmith (1994) [35]. Fig. 4 gives the results of the dislocation modelling for scenarios along the trench. Snapshots of the tsunami generation and propagation from scenario 15, over a period of 60 min are shown in Fig. 5. Fig. 5e shows the maximum elevation (m) over the domain and Fig. 5f the maximum velocity (m/s). The rupture location affects significantly the tsunami run-up due to wave directionality, as demonstrated in Fig. 6. Scenarios 01–05 (Fig. 6a), for example, have a larger impact on the eastern coast of Java (longitudes greater than 110°).

### 3. Tsunami loss calculations

#### 3.1. Socio-economic factors and vulnerability

We use a historical tsunami experience – the case of the December 26, 2004 Indian Ocean tsunami, which largely affected the Aceh province in Northern Sumatra. The corresponding household level data were collected 5–14 months after the event from around 5600 households that were used to model damage to household welfare. The data come from the first wave of the Study of the Tsunami Aftermath and Recovery (STAR1), a collaborative project involving investigators at Duke University, the University of North Carolina at Chapel Hill and SURVEY-METER [36]. Longitudinal household surveys such as STAR track the same households/individuals over time collecting information on income, consumption, livelihoods, demographic details, health, schooling and other aspects. Although the STAR project included a pre-tsunami

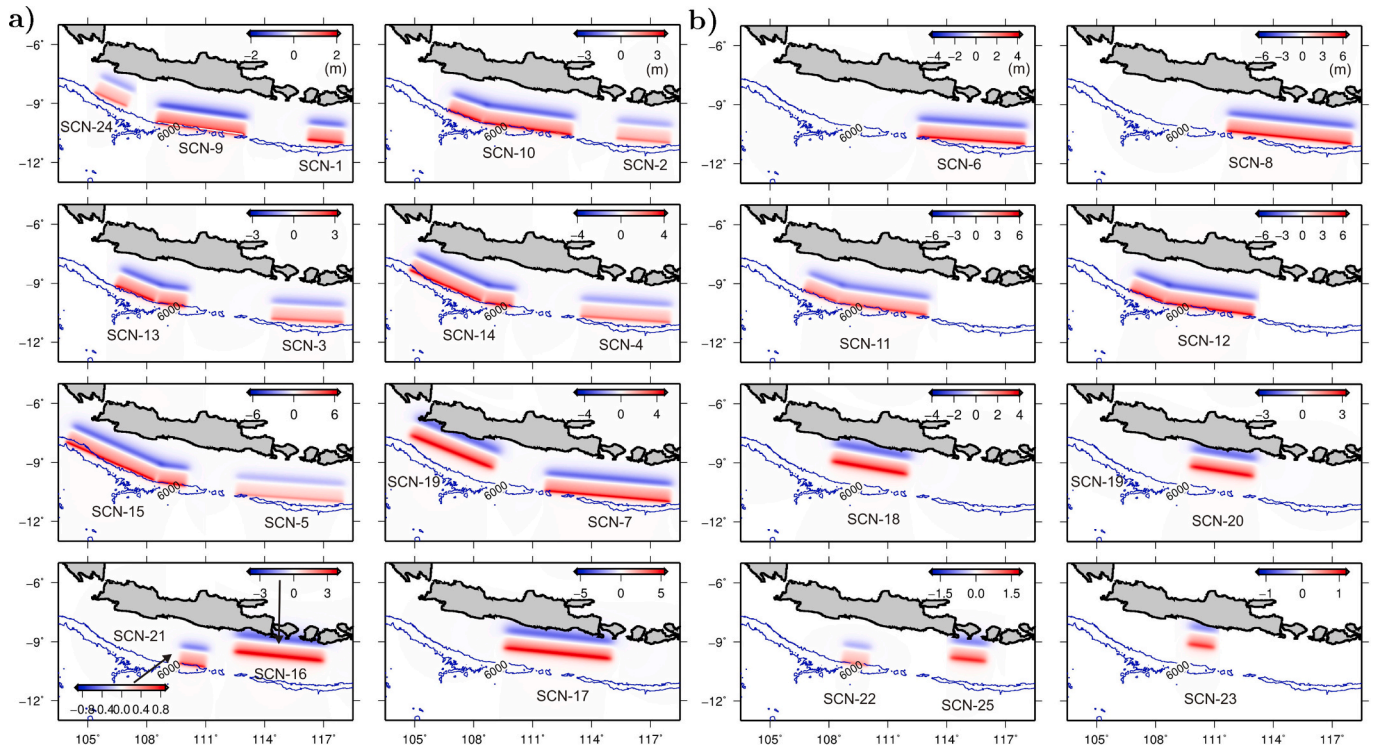


Fig. 4. The scenarios of tsunamigenic earthquakes along the Java trench. The colour bar indicates the maximum uplift and subsidence in meters for each earthquake scenario. Panel (a) shows 16 of the 25 scenarios and panel (b) shows 9 of the 25 scenarios.

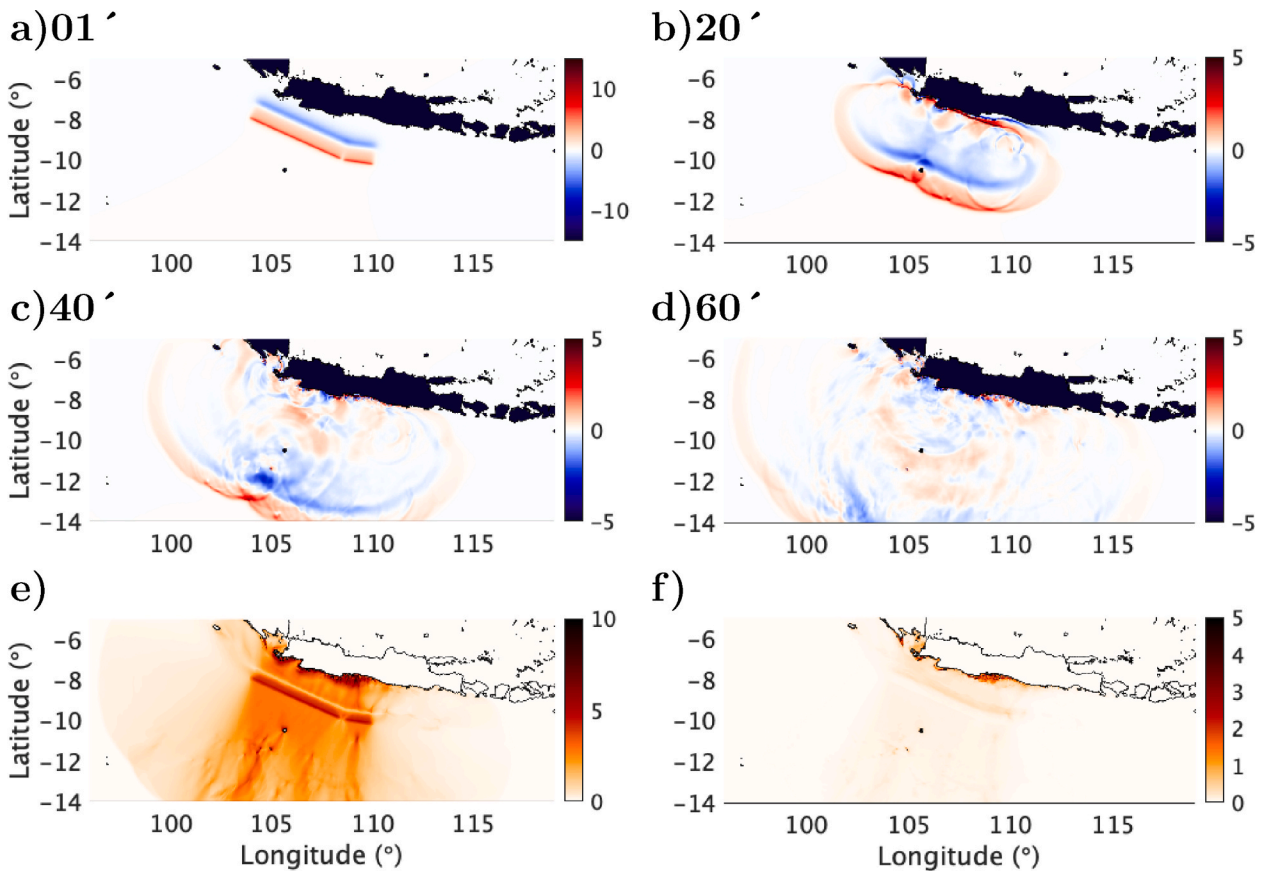


Fig. 5. a-d) Snapshots of tsunami generation and propagation from earthquake scenario 15. e) Maximum tsunami amplitude over the computational domain during the entire tsunami simulations. The colour scale is in meters. f) Maximum tsunami velocities over the computational domain during the entire tsunami simulations. The colour scale is in m/s.

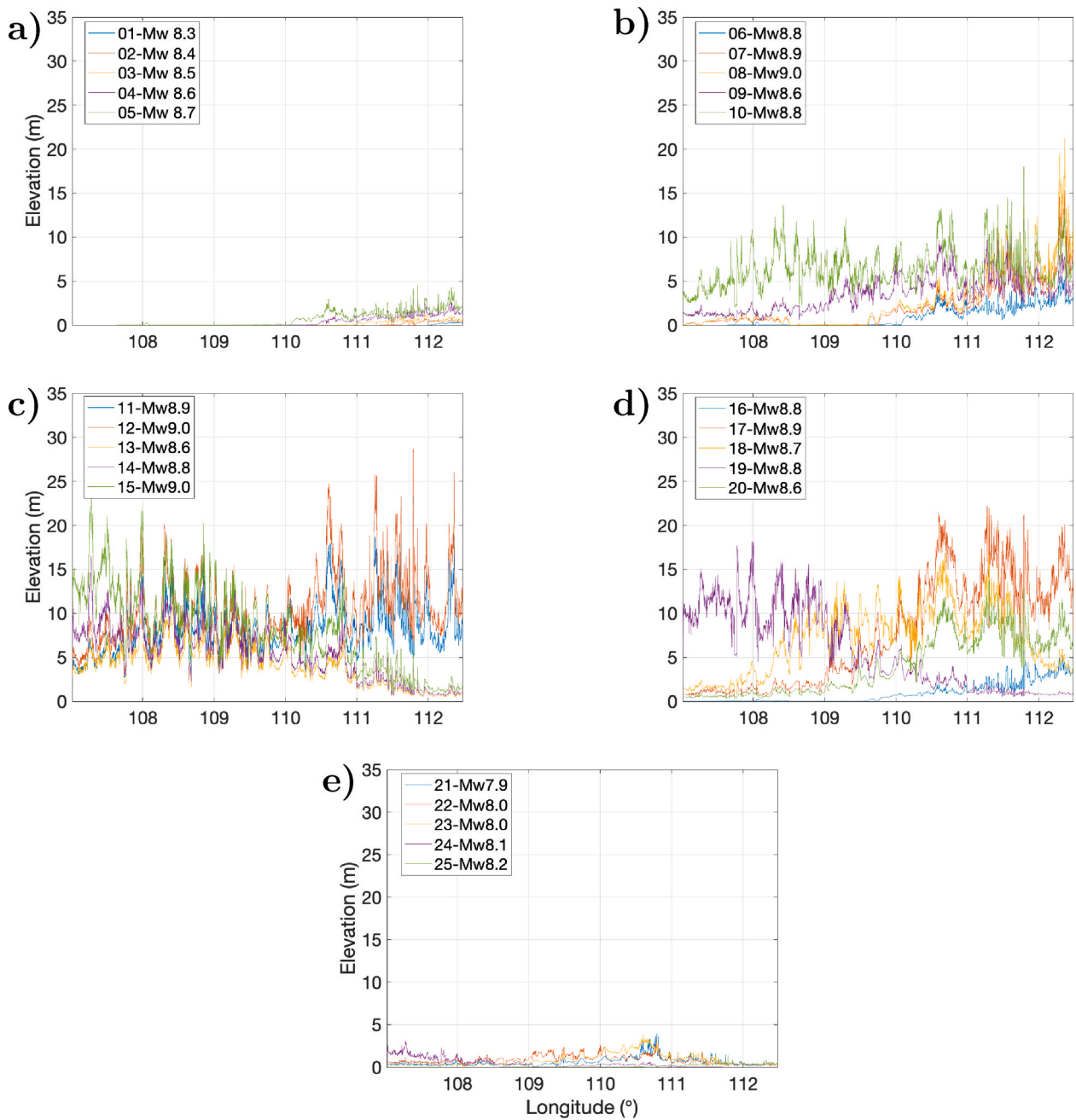


Fig. 6. Maximum wave amplitudes along the shoreline for various tsunami scenarios. The outputs are extracted from the computational grid SD02, see also locations in Fig. 2. The numbers 1–25 on the legend of the panels represent tsunami scenario numbers.

STARO survey, this has been inaccessible due to Indonesian data protection laws. Consequently the STAR1 dataset was used to obtain post-tsunami data as well as to infer pre-tsunami characteristics. The surveys gather information at several levels, from individuals, households and communities. Data collection was face to face, with enumerators travelling to the site location and being with individuals, households and community leaders, gathering data based on a pre-prepared, piloted list of instruments [36]. The respondents were usually the heads of households. Although in about 10% of the cases it was another adult. We report analysis based on responses provided by the heads of households but the results are similar with the inclusion of responses from an adult other than the head of household<sup>4</sup>.

A proxy is used for Hazard intensity: the categorical variable that describes the damage to the wider area in which a household is located. This variable is coded as heavy, moderate or light/no damage. The measure has been constructed by the STAR team, drawing on data from multiple sources including satellite imagery and Global Positioning System (GPS) measurements. For example, ‘One measure was constructed by comparing satellite imagery from NASA’s Moderate Resolution Imaging Spectroradiometer (MODIS) for December 17, 2004 to imagery for December 29, 2004 (nine days before and three days after the tsunami). The proportion of land cover that changed to bare earth between image dates (through scouring or sediment deposition) was manually assessed for a 0.6 km<sup>2</sup> area centered on each GPS point. This measure was cross-validated with other estimates of damage derived from remotely-sensed imagery that were prepared by the USGS, USAID, the Dartmouth Flood Observatory, and the German Aerospace Center’ [38]. The extent of damage was also verified through field-level data gathered from local leaders’ individual assessment of the extent of destruction to the built and natural environments in each village, as part of the community surveys in STAR1 and the survey supervisors’ direct observations.

Approximately 21% of the households were located in areas classified as experiencing heavy damage, although only 78% of these households reported that there were major losses (i.e., financial loss, death of household member, major injury or relocation due to tsunami). Around 57% of households were in medium damage areas, of which 31% experienced some form of major loss. Among the 21% households in areas with no damage or light damage, around 13% recorded some

<sup>4</sup> The sampling frame for STAR1 was based on the 2004 annual National Socio-economics Survey (SUSENAS) collected by the Indonesian Bureau of Statistics between February and March 2004. SUSENAS is a broad-purpose survey conducted across Indonesia and is representative of the population at the district (Kabupaten) level of each province. The sampling scheme for the survey is stratified, with households randomly selected within census tracts. The STAR team collaborated with Statistics Indonesia to use this as a baseline (STARO) from which to construct a panel in order to follow-up respondents from the 2004 survey. The panel sample contained all respondents living in a kabupaten with a coastline along the North and West coasts of Aceh and North Sumatra as well as the Islands off the coasts. It also contained further enumeration areas further inland that were not directly affected by the tsunami for comparison purposes [37].

form of major loss.

Were the households in areas that experienced higher damage significantly different to those in other areas? We investigate this using several pre-tsunami household characteristics derived from retrospective questions asked of households in the STAR1 survey. The characteristics include the status of the household in terms of engaging in business activity (rice farming or other farm-related business, non-farm business or no business), household wealth is captured by asset ownership<sup>5</sup> and household rural/urban location<sup>6</sup>.

As Table 1 shows, there are no significant differences in mean characteristics between households in no/light damage areas and medium damage areas. Similarly, there are no significant differences be-

**Table 1**  
Pre-tsunami household characteristics and post-tsunami outcomes. Columns 1, 2 and 3 present mean values. Columns 4 and 5 present the differences in means in medium and heavy areas, respectively, compared to no/light areas. Standard errors in brackets. \*\*\*  $p < 0.01$ , \*\*  $p < 0.05$ , \*  $p < 0.10$

	Location of household according to damage experienced in the wider area			Difference in means (standard error)	Difference in means (standard error)
	No/light	Medium	Heavy		
	(1)	(2)	(3)	(1)–(2)	(1)–(3)
<b>Pre-tsunami characteristics</b>					
Farm business (proportion)	0.435	0.454	0.397	-0.0187 (0.017)	0.0379 (0.020)
Non-farm business (proportion)	0.275	0.256	0.391	0.0190 (0.014)	-0.116*** (0.019)
No business (proportion)	0.376	0.364	0.348	0.0122 (0.016)	0.0284 (0.020)
Wealth index	0.448	0.439	0.536	0.0090 (0.006)	-0.112*** (0.006)
<b>Post-tsunami outcome</b>					
Change in asset values between 2004 and 2005 (as a percentage of asset value in 2004)	-0.039	-0.096	-0.408	0.058*** (0.006)	0.369*** (0.009)
Number of households	1174	3245	1218		

<sup>5</sup> Pre-tsunami household wealth is measured using the wealth index ranging from 0 to 1. The proxy for wealth is the household’s ownership of common assets such as a house, land, livestock, vehicles including bicycles and cars, household durable goods such as furniture and appliances, gold, cash and financial instruments such as stocks, shares and bonds. To construct the index, the list of items that household  $i$  owns is counted, regardless of its monetary value, and converted into an index as follows:  $\frac{\sum assets_i - assets_{min}}{assets_{max} - assets_{min}}$ , where  $assets_{min}$  to  $assets_{max}$  is the range of these items in the dataset. Ideally an index of wealth is a composite measure of a household’s cumulative living standards including housing quality (captured by indicators such as type roof/wall/floor type, rooms per person), the access to services (captured by indicators such as type of toilet, water source, availability of electricity) and assets (captured by durable goods such as furniture, appliances, etc). The data available in the STAR1 survey only allows us to infer the value of owned durable goods and assets such as household, land, pre-tsunami.

<sup>6</sup> A caveat here is that information is available for only post-tsunami household location. However, nearly 80% report to live in the same house as they did before the tsunami. It is assumed that the remaining 20% who moved house did so within urban areas and within rural areas, allowing us to infer pre-tsunami household rural/urban location based on post-tsunami location data.

tween households in no/light damage and heavy damage, in relation to being engaged in farming business or not engaging in household-level business activities prior to the tsunami. However, households in areas that were affected more severely by the tsunami, rather than those lightly affected, appeared to have engaged more in non-farm business activities and to be significantly wealthier. This is consistent with the result in Table 1 showing that heavy damage occurred more in urban rather than in rural areas.

Household welfare is proxied using a measure of household level business and non-business assets. The assets include farm and non-farm land, buildings, machinery and equipment, livestock, vehicles, raw material, unsold stock, hardwood trees (e.g. coconut and rubber), furniture and durable goods, gold, jewellery, cash and financial market instruments (e.g. bonds). The change in household welfare post-tsunami compared to pre-tsunami outcomes is measured using the change in the value of household-level assets. The value of pre-tsunami assets in 2004 is comprised of the total value of business and household assets held by a household before the tsunami, taken from questions asked retrospectively from respondents in this regard. The value of post-tsunami assets in 2005 are computed as the value of pre-tsunami assets in 2004 plus the value of assets lost, damaged or sold after tsunami<sup>7</sup>. All monetary values are expressed in 2007 Indonesian Rupiah adjusted for spatial variations in price<sup>8</sup>. The change in asset values between 2004 and 2005 (as a percentage of asset value in 2004) winsorized at the 1st and 99th percentiles shows that those households in heavy damage locations report a greater percentage loss of values of assets than those in areas with medium, no/light damage, at 40.8, compared to 9.6 or 3.8, respectively.

To understand the effect of the tsunami on household welfare the following baseline model is specified where the time period immediately before the tsunami is denoted by  $t = 1$  and the time period 5–16 months after the tsunami is denoted by  $t = 2$ :

$$\Delta y_{j2} = \alpha + \beta M_j + \gamma H_j + \delta X_{j1} + \varepsilon_{j2}, \tag{1}$$

for households  $j = 1 \dots N$ , where  $\Delta y_{j2}$ , which denotes the change in asset values between 2004 and 2005 (as a percentage of asset value in 2004) is the dependent variable, winsorized at the 1st and 99th percentiles.  $M_j = 1$ , if household was in an area where damage from the tsunami was moderate (0 otherwise).  $H_j = 1$ , if household was in an areas where damage from the tsunami was heavy (0 otherwise).  $X_{j1}$  is a vector of pre-tsunami household characteristics, which includes a categorical variable indicating the type of business operated by family (farming, non-farm business or no business activity) and household wealth index,  $\varepsilon_{j2}$  is an idiosyncratic shock.

Since some of the pre-tsunami characteristics are not balanced, a propensity score is estimated using baseline type of business operated by family (farming, non-farm business or no business activity) and household wealth as matching variables, and then weighting observations inversely proportional to their propensity score. This approach was adopted by Refs. [41,42]. The rationale for weighting is that samples receiving the different treatments may differ in their distributions of pre-treatment variables and, therefore, possibly differ in terms of their observed outcomes in ways that are not attributable to the treatment. If

<sup>7</sup> It is important to include the value of assets sold since the tsunami, as the sale of raw material and assets offer an important coping mechanism after natural disasters especially in cases where credit access or insurance mechanisms are weak [39,40]. Access to support may be particularly limited in the case of natural disasters as the shock is likely to be common to all members of formal or informal insurance groups. Moreover, public safety nets and aid may be inadequate, or reach victims with a time lag, leading to asset sale.

<sup>8</sup> The deflators used for this come from province-specific price indices reported by Indonesia Statistics (BPS or Badan Pusat Statistik) for 66 cities in Indonesia from 2000 to 2012 and the simple average of BPS cities Banda Aceh and Lhokseumawe are used to reflect price indices for the geographic area enumerated in the STAR survey.

all the variables with pre-treatment differences are observed and groups have at least some members with similar covariates (i.e., the conditions of conditional independence and overlap hold), then in principle, a treatment sample can be reweighted to make the distribution of covariates match that of any of the other treatment groups [43,44]. The identifying assumption in the model is that  $E(\varepsilon_{j2} | M_j, H_j, X_{j1}) = 0$ , so that tsunami intensity, household business activity and wealth status in 2004 are not correlated with unobservables determining asset loss between 2004 and 2005. Identification relies on the exogenous nature of the tsunami.

The issue of internal validity is important when estimating hazard relationships [45]. This refers to the establishment of a causal (or, at least, externally replicable) relationship between tsunami intensity and household welfare loss. The main measure of tsunami intensity in the above specification is the damage indicator rather than measures of wave height or force as it reached a particular household. Although damage is the most direct measure of the tsunami intensity available, measured at roughly 0.6 km<sup>2</sup>, there are two key disadvantages with the measure. First, it is not nuanced enough to capture the finer grades of intensity. For example, around 50% of the households are in the ‘moderate’ damage area. Second, damage extent may be correlated with unobserved determinants of asset loss. For example, if wealthier, urban areas indicate heavier damage but also have a more diverse portfolio of assets qualitatively different to those of more rural areas with assets (e.g.

**Table 2**  
Impact of tsunami on household-level assets conditioned on pre-tsunami characteristics, using Ordinary Least Squares estimation, with standard errors in brackets. The columns (1), (2) & (3) represent different specifications: (1)-all controls apart from rural, (2)-all controls and (3)-parsimonious (used in OASIS). \*\*\*  $p < 0.01$ , \*\*  $p < 0.05$ , \*  $p < 0.10$  Dependent variable:  $\Delta y_{j2}$ .

	(1)	(2)	(3)
medium	-0.0580*** (0.0053)	-0.0581*** (0.0052)	-0.0578*** (0.0074)
heavy	-0.330*** (0.0106)	-0.337*** (0.0111)	-0.375*** (0.0090)
farm	-0.0399*** (0.0128)	-0.0215 (0.0136)	
nonfarm	-0.0393*** (0.0121)	-0.0380*** (0.0122)	
nobusiness	-0.0147 (0.0158)	-0.00806 (0.0160)	
wealth	-0.155*** (0.0196)	-0.156*** (0.0199)	
rural		-0.0280*** (0.0088)	-0.0319*** (0.0064)
Constant	0.0667*** (0.0159)	0.0778*** (0.0166)	0.0144* (0.0081)
Observations	5,637	5,637	5,637

gold, stocks, shares, bonds) kept in banks rather than at home (causing lower levels of asset loss for a given tsunami intensity), then there would be an over-estimation of the welfare loss of tsunami in these areas. To deal with this, we include observable pre-tsunami characteristics in the specification but acknowledge that unobservable characteristics, that may influence both the proxy for intensity and welfare loss, remain unaccounted.

The results of the Ordinary Least Squares estimation of Eq. (1) are presented in Table 2, Column 1. They show that a household that was in an area of medium damage rather than no/little damage reduced its welfare significantly by 5.8%. Households that were in a heavy damage area rather than a no/little damage area showed welfare losses of 33%. Household business type (farm or non-farm) and wealth had significant negative impacts on asset loss.

To test for internal validity (weakly stated as robustness of tsunami-welfare loss over different specifications), Eq. (1) was re-estimated as follows: (a) Include an indicator for rural/urban residence in the



specification and change the propensity score weight to include this dummy (b) present a parsimonious specification including only the rural/urban dummy and an estimate unweighted regression (c) Employ the non-parametric nearest-neighbor matching estimator [46] to obtain the average treatment effects (ATE) as well as average treatment effects on treated (ATT)<sup>9</sup>. The results for the first two checks for robustness are reported in Table 2, Columns 2 and 3, respectively. The ATEs from the matching estimator are 5.8% and 34.9%, respectively, for medium and heavy intensity. The corresponding ATTs are 5.8% and 36.5%. Thus the results remain robust to changes in specification and the use of a non-parametric estimator: medium tsunami intensity significantly reduces household welfare by 6% in all cases while heavy intensity reduces household welfare significantly by 33–37.5%.

Are these results externally valid i.e., generalizable out of sample in other contexts, locations or years such as for the case of Cilacap that may have a different development profile? This is a difficult question to answer. First, the empirical measurement of direct and indirect micro-economic losses in the context of a disaster is still a nascent field in economics and related social sciences, and there is much work yet to be done. Thus the relationship between different socio-economic contexts and vulnerability in the face of a disaster is far from clear. Second, major disasters often result in countries subsequently changing policy. Endogenising this type of political response in a model is particularly difficult and may require the subjective judgement of analysts. Most importantly, estimates based on past experience may never guarantee similar behavior in the future as contexts change over time [45]. In spite of these difficulties in establishing external validity, we attempt to contextualize our results for Aceh by considering the case of a major disaster in another location in Indonesia. An ideally suited event to consider is the 2006 Pangandaran tsunami affecting South Java including Cilacap. Although we have another household panel data set, the Indonesian Family Life Survey (IFLS) [50] to use for this purpose, it captures only around 25 households that experienced the 2006 tsunami and therefore provides a sample size too small for empirical analysis. So the IFLS data are used to estimate the impacts of the May 27, 2006 Yogyakarta earthquake that recorded a 6.6 magnitude and Medvedev–Sponheuer–Karnik scale of VIII (damaging). Tsunami damage to household assets can be more severe than earthquake damage, given that flooding affects land, livestock and other assets more severely [51]. Nonetheless, the results may offer some insights as to how plausible the 2004 tsunami based results on our measure of assets may be, in the Indonesian context. Waves 3 and 4 of the IFLS dataset collected in 2000 and 2007 are used to look at the impact of the Yogyakarta earthquake on household welfare<sup>10</sup>. The earthquake struck near the city of Yogyakarta,

<sup>9</sup> The effect of tsunami on welfare obtained from Eq. (1) can be interpreted as the average treatment effect (ATE), using terminology from the potential outcomes literature [47]. The ‘treatment’ is tsunami intensity, that has three levels-no/light, medium and heavy. The same results can be obtained using the inverse probability weighting with regression adjustment (IPWRA) estimator as described in Refs. [48,49] with the estimation procedure rewritten as a one-step step estimation within a Generalised Method of Moments (GMM) framework such that the standard errors automatically account for the estimation error from estimated propensity scores. Using the potential outcome framework also allows us to compute the average treatment effect on the treated (i.e., the mean effect for those who actually received the treatment) rather than the average treatment effect (the mean effect of giving each individual treatment heavy or medium instead of treatment no/light treatment). ATEs and ATTs can differ when the treatment effects are not constant across individuals (i.e., there exists treatment effect heterogeneity). The ATEs and ATTs can be obtained using an alternative non-parametric estimator as well such as nearest neighbor matching using the Mahalanobis distance metric.

<sup>10</sup> The first wave of the IFLS was collected in 1993, with the sample representative of 83% of the Indonesian population. Subsequent rounds of data were collected for the full sample over the next 20 years in 1997, 2000, 2007 and 2014.

incurring substantial damage to buildings, assets and housing. The measure of earthquake intensity used is the number of houses destroyed per capita (at the district-level) by the earthquake. This variable is continuous ranging from 0 to 0.091, rather than being categorical as was the proxy for tsunami intensity<sup>11</sup>. The measure of changes in household welfare is computed using changes to household level business and non-business assets, using pre and post-disaster data. In this case the pre-disaster data pertain to the year 2000 and post-disaster data to the year 2007, gathered roughly 18–25 months after the 2006 earthquake. Effects are identified using a specification similar to Eq. (1) above, with the change in household assets between 2000 and 2007 regressed on pre-earthquake characteristics that include business type (farm, non farm, no business), wealth and location<sup>12</sup>. Since some of the pre-earthquake characteristics are not balanced, the observations are weighted using inverse probability weights, as for the tsunami-based regression.

The results (unreported) indicate that the average effect of the earthquake is to reduce household welfare significantly by 28.9%. It should be noted, however, that the earthquake effect is likely to be an overestimation for two reasons. First, the measure of intensity is available only at the district level. Secondly it may be correlated with unobserved determinants of asset change. For example, housing quality may be lower in poorer areas resulting in higher levels of destruction for a given magnitude. If these areas also had lower asset growth, the effect of the earthquake will be overestimated. Nonetheless, the average impact of the earthquake of reducing household welfare by 28.9% is between the previous tsunami impact estimations of 6% and 37.5% for medium and heavy areas, respectively, compared to light/no damage areas. This result supports somewhat the observation that the effects of flooding can be more damaging for household assets than earthquakes. It also supports to some extent the notion that the Aceh-based estimations are plausible in a different context within Indonesia. However, it is acknowledged that further research in this area is needed to ensure that the results are externally valid.

### 3.2. The Oasis loss framework

Catastrophe models have been widely employed by the (re-)insurance businesses and government sectors to assess the risks posed by natural hazards and estimate the prospective losses. There is an increasing need for transparency within the (re-)insurance community, and beyond, especially relating to the black-box use and design of

<sup>11</sup> Authors gratefully acknowledge data shared by Martina Kirchberger, from her paper [42], that was useful in capturing effects of the Yogyakarta earthquake. As the paper noted, the data for reported earthquake damage to households came from the DesInvestar database for Indonesia, maintained by the Indonesian National Board for Disaster Management. District-level population data for 2005 were taken from Indonesia’s Statistical Agency. The paper also contains more details on how treatment and control groups were carefully assigned, restricting the sample to households within a Euclidean distance of 5 km of cities with a population of more than 300,000 people in Java in 2000.

<sup>12</sup> Unlike the STAR data set, the IFLS allows us to calculate a more complete wealth index using pre-disaster data similar to the method used in papers such as [52]. Thus the wealth index in this case is calculated as the simple average of three sub-indices: the housing quality index, the access to services index and the asset index. The housing quality sub-index reflects the welfare of household members in terms of housing-related comfort and is the simple average of the four indicators based on wall, roof, floor quality and rooms per person. The access to services sub-index measures the household’s ability to meet functional requirements of sound shelter. Again it is calculated as the simple average of four indicators: access to electricity, safe drinking water, safely managed sanitation Service and adequate fuel for cooking. All four indicators are considered to have equal weight. The consumer durables sub-index is a measure of the household’s ownership of common household durable goods and assets (such as TV, radio, bicycle, cars). It counts a long list of items (regardless of its monetary value) that the household has and converts it into an index.

catastrophe models. In an attempt to provide with more transparency the Oasis Loss Modelling Framework (LMF), an open source catastrophe modelling platform, was created<sup>13</sup>. Several components are integrated in the core/kernel of Oasis to calculate ground-up losses. Overall, three main components are distinguished with reference to the hazard, vulnerability and financial structure (see also Fig. 7). Event occurrences and exposure data are also incorporated in the model. Ground-up losses are calculated through Monte Carlo sampling. In the following paragraphs we discuss the different model choices that led to the computations of the tsunami loss exceedance curves for the area of Cilacap.

### 3.2.1. Hazard

Hazard in Oasis is represented by the hazard footprints of a set of events. In this study, the hazard footprints describe the numerical outputs of the 25 tsunami event set (expressed as tsunami maximum elevation over the whole disaster duration) for the population distribution data of Cilacap. The intensity of the events is divided into three intervals depending on the expected impact of the maximum tsunami elevation on the population (small/no impact, medium or high impact). This classification is driven by the damage classification of the 2004 tsunami in the Aceh province, Indonesia. We assume the threshold between light to medium intensity to vary among 0.2–1 m and the threshold between medium to heavy damage to vary among 1–5 m<sup>14</sup>. We sample randomly from these intervals and produce 1,000 instances for which we run the model in order to express our own uncertainty over the threshold values.

### 3.2.2. Occurrences

In Oasis the occurrences of events are expressed as a series of identified tsunamis over time. To create this event set we use a simple approach that combines a frequency/magnitude relationship with a Poisson distribution of inter-event times. Earthquake frequency-magnitude relationships can often be described by the Gutenberg-Richter (GR) law [53]. The GR law expresses the number of earthquakes of a certain magnitude, or higher, that may occur in a region within a specific time period. Based on the historical seismicity of the region between 1977 and 2011, Okal [16] has estimated this relationship to be:  $\log_{10}N = 16.7 - 0.62\log_{10}M_0$ , where  $N$  is the number of events with a seismic moment  $\geq M_0$ . The regression was based on data that ranged between  $10^{24}$  and  $6 \times 10^{25}$  dyn.cm. Extrapolating this

relationship, a megathrust event ( $M_0 \geq 10^{29}$  or  $Mw \geq 8.6$ ) would occur roughly every 670 years [16]. Following the same approach, we estimate the expected time intervals for each one of the 25 earthquake scenarios. Thus, in a period of 297,470 years 10,000 events with  $Mw$  7.9–9 could occur, out of which 19.85% would have a  $Mw$  7.9 and 2.1% would have a  $Mw$  9.

To distribute events over time we employ the Poisson distribution. The distribution of inter-event times behaves exponentially with parameter  $\lambda$ , the mean rate of events per interval. The distribution of the inter-event time intervals ( $\delta_i$ ) until the next earthquake of/larger than a certain magnitude is expressed by:  $P(\delta_i < t) = e^{-\lambda t}$ . The Poisson model has been widely used in the past for probabilistic seismic hazard analysis, however in modern earthquake statistics it is considered the “least-informative” model as it assumes independence and randomness amongst the main-shocks and a stationary seismic process. We nevertheless follow this approach in this study for its simplicity and efficiency in the lack of additional information other than the mean rate of earthquake generation (its concrete impact in Oasis computations is negligible as averages as aggregated after Monte Carlo sampling anyway). We thus sample randomly 10,000 inter-event times with a rate  $\lambda$  corresponding to each mean recurrence rate for the corresponding magnitude and attribute the set of earthquake events to these intervals according to frequencies derived from the GR law.

As a result, these 10,000 events are distributed within 297,470 years. Fig. 8a displays one possible set of occurrences in time according to magnitude, showing for instance six  $Mw$  9 events in 10,000 years in this draw. We generate 6 sets of inter-event times to assess the impact of such random variations. Note that a recent study [54] showed that for the 2004 tsunami was the latest in a sequence of tsunamis along the Sunda Megathrust. This investigation established that the average time period between tsunamis is about 450 years with intervals ranging from a long, dormant period of over 2000 years, to multiple tsunamis within the span of a century. Hence the large variability in actual recurrence suggests that it is informative to consider events with large return periods with care in their statistical representation. Note that we do not capture such variability here with our stationary behaviour in time (see Fig. 9).

### 3.2.3. Vulnerability

For Oasis purposes, a variation of the tsunami vulnerability function discussed previously is used by making the dependent variable categorical. For simplicity we also use only hazard intensity and location of household (rural versus urban) as explanatory variables. An econometric model is built here, which predicts how much loss each household would incur depending on the values of explanatory variables. After constructing it, we estimate the parameters of the model based on the historical data and use the model for future prediction. We employ a multinomial logit model (see for example [49]) and the formulation is reviewed. First, we classify the degree of loss into the six categories (Table 3). For each individual household  $i$ ,  $y_i$  denotes a random variable taking on the values  $\{1, 2, 3, 4, 5, 6\}$  and it specifies into which category the loss incurred by household  $i$  falls.

The explanatory variables are a constant and dummy variables  $d_{i,rural}$ ,  $d_{i,medium}$ ,  $d_{i,heavy}$ .  $d_{i,rural}$  takes 1 if the location of household  $i$  is rural.  $d_{i,medium}$  and  $d_{i,heavy}$  are equal to 1 if the household  $i$  experiences medium or heavy tsunami intensity respectively. Then, the probability that the loss of household  $i$  is classified into category  $j$  is:

$$P(y_i = j) = \frac{\exp(\beta_{0,j} + \beta_{1,j}d_{i,rural} + \beta_{2,j}d_{i,medium} + \beta_{3,j}d_{i,heavy})}{1 + \sum_{h=2}^6 \exp(\beta_{0,h} + \beta_{1,h}d_{i,rural} + \beta_{2,h}d_{i,medium} + \beta_{3,h}d_{i,heavy})} \quad (2)$$

where  $j = 2, \dots, 6$  and the probability for  $j = 1$  is:

$$P(y_i = 1) = \frac{1}{1 + \sum_{h=2}^6 \exp(\beta_{0,h} + \beta_{1,h}d_{i,rural} + \beta_{2,h}d_{i,medium} + \beta_{3,h}d_{i,heavy})} \quad (3)$$

The log likelihood can be written as:

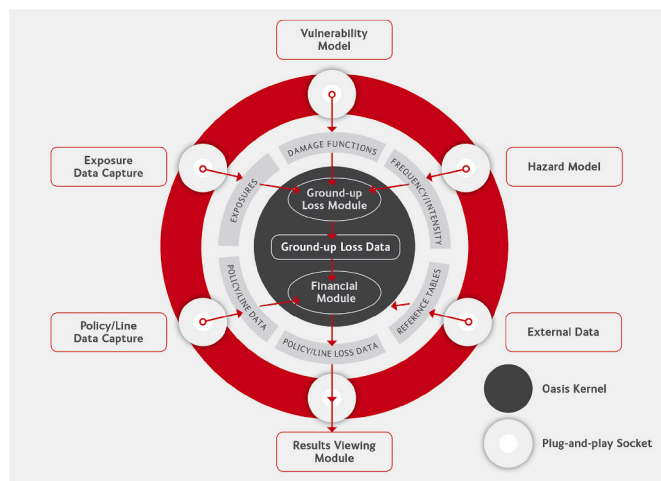
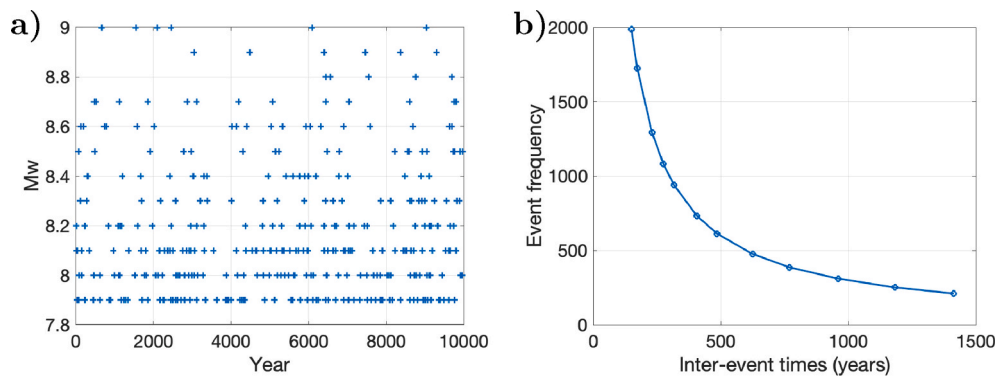


Fig. 7. The Oasis Loss modelling framework.

<sup>13</sup> <https://github.com/OasisLmf>.

<sup>14</sup> Note, these values correspond to tsunami height as opposed to inundation depth.



**Fig. 8.** (a) Distribution of events with varying moment magnitudes over a subset (10,000 years) of the total time. (b) Distribution of the 10,000 events along the inter-event times that result from the GR law.

**Table 3**

Classification of the incurred loss (negative change in household asset and business asset values).

Category	1	2	3	4	5	6
Loss interval	[0, 0.05]	(0.05, 0.2]	(0.2, 0.4]	(0.4, 0.6]	(0.6, 0.8]	(0.8, ∞)

$$L(\beta) = \sum_{i=1}^N \sum_{j=1}^6 1_{(y_i=j)} \log(P(y_i=j)) \quad (4)$$

where  $N$  means the total number of samples (in our case  $N = 6,277$ ) and  $\beta$  denotes the set of  $\beta_{lj}$  for  $l = 0, 1, 2, 3$  and  $j = 2, \dots, 6$ . We estimate  $\beta$  by maximum likelihood method and all of  $\beta_{lj}$  are significant with a significance level 0.001 except for  $\beta_{2,5}$ , which is still significant with a significance level 0.01 (Table 4).

Using the expressions in Eqs. (2) and (3) with the estimated parameters of  $\beta_{lj}$ , we can compute the probability of loss for a new household  $m$  in Cilacap. The value of the corresponding explanatory variable  $d_{m,rural}$ , which is interpreted as exposure, is set to 0, which means the location of every household in Cilacap is considered as an urban area while  $d_{m,medium}$  and  $d_{m,heavy}$  take 0 or 1 depending on the simulated value of tsunami. In Table 5, the probability that specifies the loss of household  $m$  is presented. This is used as a vulnerability file in Oasis framework. If  $d_{m,heavy} = 1$ , the intensity experienced by the household  $m$  is heavy whereas  $d_{m,medium} = 0$  means the household  $m$  incurs medium intensity. The Light column in Table 5 corresponds to the case where  $d_{m,heavy} = 0$  and  $d_{m,medium} = 0$ . The values of  $d_{m,medium}$  and  $d_{m,heavy}$  change according to the tsunami height in different scenarios and this vulnerability file allows us to specify the corresponding probability. More intense tsunamis generate a higher likelihood of experiencing a higher loss (categories 5 & 6 in particular). There is

**Table 4**

Estimated parameters with standard deviations.

$\beta_{0,2}$	$\beta_{0,3}$	$\beta_{0,4}$	$\beta_{0,5}$	$\beta_{0,6}$
-3.38 (0.16)	-4.23 (0.21)	-4.56 (0.26)	-4.53 (0.26)	-5.40 (0.38)
$\beta_{1,2}$ 0.42 (0.11)	$\beta_{1,3}$ 0.68 (0.12)	$\beta_{1,4}$ 0.57 (0.13)	$\beta_{1,5}$ 0.46 (0.12)	$\beta_{1,6}$ 0.54 (0.16)
$\beta_{2,2}$ 0.96 (0.15)	$\beta_{2,3}$ 1.37 (0.20)	$\beta_{2,4}$ 1.19 (0.25)	$\beta_{2,5}$ 0.83 (0.25)	$\beta_{2,6}$ 1.24 (0.38)
$\beta_{3,2}$ 2.03 (0.18)	$\beta_{3,3}$ 2.97 (0.21)	$\beta_{3,4}$ 3.65 (0.25)	$\beta_{3,5}$ 4.11 (0.25)	$\beta_{3,6}$ 4.24 (0.37)

**Table 5**

Estimated distributions, from the multinomial logit regression model, of loss categories defined in Table 3, by tsunami intensity classification (so columns sum to 1).

Category	Heavy	Medium	Light
1	0.3423	0.8189	0.9307
2	0.0890	0.0727	0.0318
3	0.0974	0.0470	0.0135
4	0.1372	0.0282	0.0097
5	0.2262	0.0203	0.0100
6	0.1078	0.0128	0.0042

nevertheless a large percentage of households experiencing no or less than 5% losses for all intensities (e.g. 34.23% for heavy tsunamis), possibly due to more resilient assets with stronger defences, or types of assets less affected by tsunamis for such households.

### 3.2.4. Exposure

Exposure in Oasis is represented by the coverage that each item has with reference to a total insured value (TIV). The items' TIVs are defined by the average asset value in each sub-district after subtracting the percentage that is already insured (and thus covered by another source). The estimated values for assets for each of the districts in Cilacap are obtained from the Indonesia Family Life Survey, wave 5 (IFLS5), conducted in 2014. The asset-related survey instruments of the IFLS5 are comparable to that of STAR1, and include household-level business and non-business assets. Although the IFLS5 obtained information for around 70,000 households in total, these households were distributed across 13 provinces in Indonesia, each comprising many regencies. Thus, only a few households in coastal Cilacap were included in the sample<sup>15</sup>. The calculated TIVs are shown in Table 6. All vehicles are assumed to be insured and thus insured assets as a percentage of total assets is presented in the last column. The number of households obtaining insurance against buildings and other assets is negligible in Indonesia's case. Each item is characterised by a coverage ID, incurred from their sub-district TIVs, the area peril ID (household location) and a vulnerability ID (which is the same for all households). The items are grouped together and used in the calculations of the ground-up losses.

<sup>15</sup> Household surveys such as the IFLS are most useful to identify patterns, causes and consequences, rather than be used for monitoring purposes, as would a population based census. Although population based data on assets would have been ideal for the current investigation, such detailed data is unavailable and can only be obtained through a household survey such as the IFLS.

**Table 6**

The estimated asset values in the sub-districts of Java as given by the IFLS 2014 survey. The values are given in 2014 rupiah prices. The insured assets as of 2014 are also given. The total insured value is estimated using these values as a guideline. Source: Indonesia Family Life Survey 2014.

Sub-district	Surveyed households	Average asset value/household	Insured assets	%assets insured	Total Insured value
Jeruklegi	1	$3.8 \times 10^7$	$1.05 \times 10^7$	27.63	27,500,600
Kesugihan	3	$1.43 \times 10^8$	$5.233 \times 10^6$	3.66	137,766,200
Adipala	4	$2.35 \times 10^8$	$6.375 \times 10^6$	2.71	228,631,500
Cilacap Selatan	4	$2.44 \times 10^8$	$3.28 \times 10^7$	13.44	211,206,400
Cilacap Tengah	37	$4.49 \times 10^8$	$5.87 \times 10^7$	13.07	390,315,700
Cilacap Utara	4	$4.66 \times 10^8$	$5.41 \times 10^7$	11.61	411,897,400

**3.2.5. Financial**

In general, there are many ways to compute an insurance loss, under a range of different terms and conditions. For instance, there may be deductibles applied to each element of coverage (e.g. a buildings damage deductible), some site-specific deductibles or limits, and some overall policy deductibles and limits. The financial module in Oasis is intended to incorporate these aspects. The financial module links the varying (re-)insurance policies with the hazard impact, see Fig. 7. It comprises several components that relate to different financial layers and the contracts/policies that should be applied under each condition. Financial terms and conditions are represented in Oasis by three main files: FM Programme, FM Profile and FM Policy. The FM Programme describes the hierarchical aggregation of financial structures and the FM Profile specifies the calculation rules and the values to be used. The FM Policy connects the hierarchical aggregation structure to the profile and also describes any insurance layer conditions. In our case, we do not assume specific terms, and thus do not modify the computed loss, and thus all losses from individual households are summed up to one final output.

**3.3. Loss exceedance curves**

Loss exceedance curves (LECs), also called exceedance probability (EP) curves, form a predominant indicator of risk as they express the loss expectancy over a future period. More specifically, LECs graphically represent the probability that a certain amount of economic loss will be exceeded over a given time interval. LECs are computed by combining of different elements such as hazard, vulnerability, exposure and financial aspects, through Monte Carlo sampling (see Fig. 7). Tsunami events are generated in time, and the corresponding footprints are used to determine the intensity of impact onto each household. Then a probability of falling into a category of loss is sampled for each household using Table 5 and used to reduce the household assets in Table 6 by a corresponding proportion from Table 3. The totals are aggregated into the overall losses, the so-called ground up losses. As time increases, these losses increase and may increase at a different rate as low probability but high impact tsunamis appear in the time window. The resulting LECs for Cilacap are shown in Fig. 10. We calculate the LECs for 1,000 times, with different hazard intensity thresholds at each iteration, for one set (out of the six) of 10,000 inter-event times that span across 297,470 years. The LECs in Fig. 10 represent a subset of 100 out of the 1,000 calculations.

**Table 7**

Earthquake scenarios used as source in the tsunami simulations, All scenarios have a fault width of 100 km. Rigidity of earth is assumed to be  $3 \times 10^{10}$  (N/m<sup>2</sup>) after Fujii and Satake [11].

Scena-	Lon/Lat	Length (km)	Depth (km)	Slip (m)	Max uplift (m)/	M <sub>0</sub> (dyne. cm)	Mw
rio					Max sub (m)		
01	118.0/-11.0	200.0	8.0	5.0	2.0/-1.1	$3.00 \times 10^{28}$	8.3
02	118.0/-11.0	300.0	8.0	5.0	2.0/-1.1	$4.50 \times 10^{28}$	8.4
03	118.0/-11.0	400.0	8.0	5.0	2.0/-1.1	$6.00 \times 10^{28}$	8.5
04	118.0/-11.0	500.0	8.0	6.0	2.4/-1.3	$9.00 \times 10^{28}$	8.6
05	118.0/-11.0	600.0	8.0	7.0	2.8/-1.6	$1.26 \times 10^{29}$	8.7
06	118.0/-11.0	600.0	8.0	10.0	4.0/-2.3	$1.80 \times 10^{29}$	8.8
07	118.0/-11.0	700.0	8.0	12.0	4.8/-2.7	$2.52 \times 10^{29}$	8.9
08	118.0/-11.0	700.0	8.0	16.0	6.4/-3.6	$3.36 \times 10^{29}$	9.0
09	113.0/-10.6	500.0	8.0	6.0	2.4/-1.3	$9.00 \times 10^{28}$	8.6
10	113.0/-10.6	500.0	8.0	9.0	3.6/-2.5	$1.89 \times 10^{29}$	8.8
11	113.0/-10.6	200.0	8.0	9.0	108.4/-9.93		
11	113.0/-10.6	500.0	8.0	12.0	4.8/-3.4	$2.52 \times 10^{29}$	8.9
12	113.0/-10.6	200.0	8.0	12.0	108.4/-9.93		
12	113.0/-10.6	500.0	8.0	16.0	6.4/-4.5	$3.36 \times 10^{29}$	9.0
13	110.0/-10.2	500.0	8.0	8.0	3.2/-2.0	$9.6 \times 10^{28}$	8.6
14	110.0/-10.2	200.0	8.0	8.0	108.4/-9.93		
14	110.0/-10.2	160.0	8.0	10.0	4.0/-2.7	$1.8 \times 10^{29}$	8.8
14	110.0/-10.2	440.0	8.0	10.0	108.4/-9.93		
15	110.0/-10.2	160.0	8.0	16.0	6.4/-4.4	$3.36 \times 10^{29}$	9.0
15	110.0/-10.2	540.0	8.0	16.0	108.4/-9.93		
16	117.0/-10.0	500.0	16.0	10.0	3.9/-2.2	$1.80 \times 10^{29}$	8.8
17	115.0/-9.9	600.0	16.0	14.0	5.4/-3.1	$2.52 \times 10^{29}$	8.9
18	112.0/-9.6	430.0	16.0	10.0	3.9/-2.2	$1.29 \times 10^{29}$	8.7
19	109.0/-9.3	500.0	16.0	12.0	4.6/-2.6	$1.80 \times 10^{29}$	8.8
20	113.0/-9.7	360.0	16.0	8.0	3.1/-1.7	$8.64 \times 10^{28}$	8.6
21	111.0/-10.3	150.0	8.0	2.0	0.8/-0.4	$9.0 \times 10^{27}$	7.9
22	110.0/-10.2	150.0	8.0	2.5	1.0/-0.5	$1.13 \times 10^{28}$	8.0
23	111.0/-9.3	150.0	16.0	2.5	1.0/-0.5	$1.13 \times 10^{28}$	8.0
24	107.0/-9.15	200.0	8.0	3.0	1.2/-0.6	$1.8 \times 10^{28}$	8.1
25	116.0/-10.0	200.0	16.0	4.0	1.6/-0.8	$2.4 \times 10^{28}$	8.2

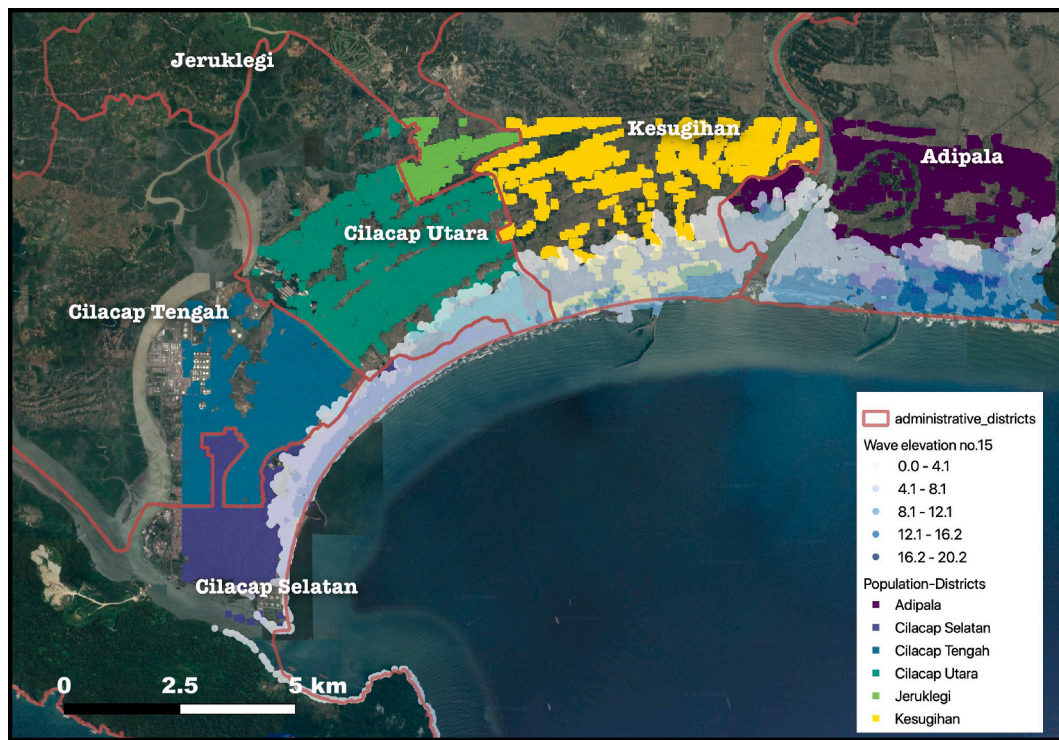


Fig. 9. Population data are classified on a sub-district level. The maximum elevation as modelled from scenario 15 is also presented (units are in metres). The map is produced with the QGIS software using as base-maps the Google satellite layers.

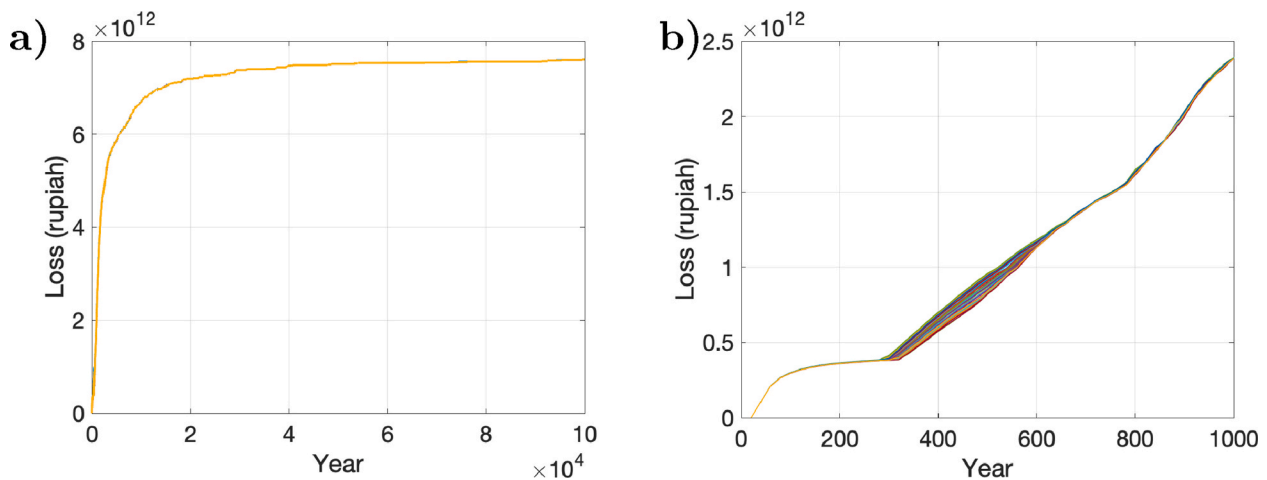


Fig. 10. Loss exceedance curves over the next 100,000 years (a) and over the next 1,000 years (b), the results are shown for one out of six catalogues of inter-event times. The loss is calculated in rupiah. An ensemble of 100 of these curves according to the tsunami intensity thresholds is employed in both panels but is only visible on the right panel.

4. Discussion

The Loss Exceedance curve in Fig. 10 shows a sharp rise and then a plateau of around  $7 \times 10^{12}$  Indonesian rupiahs or roughly 483 million U. S. dollars. This plateau is reached very late in terms of occurrences at a return period of 20,000 years. Fig. 10b focuses on the period up to 1,000 years and illustrates that losses start to increase for events with return periods beyond 20 years. The Oasis calculations estimate losses at the rates of approximately  $1 \times 10^{11}$  rupiahs for events with return periods of 40 years. These losses increase more sharply beyond 250 years due to much larger losses when the magnitudes of the tsunamis intensify. The LECs show that the variance we set in the hazard intensity thresholds does not have a substantial impact on the overall trend of the loss

calculations; it is nevertheless noticeable for events with periods between 250 and 600 years (Fig. 10a–b). The concerns of policy makers will likely be centered around 200–1,000 year return periods or so, corresponding to tsunamis such as Sumatra 2004 or Tohoku 2011 and smaller ones. Direct losses of household and business assets represent a value of around  $0.5 \times 10^{12}$  to  $2.5 \times 10^{12}$  Indonesian rupiahs or roughly 34–170 million U.S. dollars, sufficient to destabilize the local economy in the short and medium term.

There are several limitations in our calculations. The loss calculations could benefit from a more informative event set, as for example with a larger variance amongst intermediate earthquake magnitudes. Uncertainties in the ranges of exposures are not included as initial assets estimates are often based on one point estimate per district. The

exposure is not fully matched with inundation limits, although substantial care was given in achieving the appropriate match, using respectively 28 m and 30 m resolution grids for exposure and tsunami footprints that were overlaid. Finally, the incorporation of more precise information about the region's socioeconomic data can potentially lead to a more encompassing analysis of the future tsunami risk.

As this study is the first to present such calculations relating tsunami modelling, household data, microeconomic indicators, statistical modelling and the Oasis platform, some aspects have been simplified to focus on the most novel aspects pertaining to household welfare. In particular, future investigations may be focused on a wider range of possible future tsunami footprints, over a larger region, not limited (due to the prohibitive cost of running a large number of simulations at high resolutions over large areas) to a discrete set of 25 events and inundation only for the city of Cilacap. To account for that, the nascent leading approach has been to run the computer model over a small design of experiments and use this to create a surrogate, also called an emulator. Such an approach requires care in the design and the process of emulation (e.g. the parameterisation of the source), but has already shown success in various regions, such as Cascadia, NE Atlantic and the Western Indian Ocean [23,55–57]. An important source of uncertainties is the bathymetry in the coastal areas that have not been thoroughly surveyed; for Indonesia and other countries with extremely long and complex coastlines, it can be a challenge. In terms of the vulnerability module, improved analysis could be performed to contextualize and confirm the external and internal validity of the computations.

Finally, there is the potential for policy-makers to design either insurance schemes or welfare systems that can mitigate the economic shock created by the disaster. There are now highly probable for tsunamis with the approach outlined. Optimising schemes can lead to improved efficiency and cost benefits. For instance, the Oasis framework, see Fig. 7, allows for excesses and limits to be included in its financial module, though none were used any in the modelling above. For instance, such allowances can be used to restrict the payments to the most impacted households, limiting settlements and targetting the poorer ones. Also in the vulnerability module, the measure of household welfare can be varied to include longer term impacts on aspects such as mental and physical health and education. Doing so would enable a more holistic capture of the welfare effects of the tsunami, aiding the understanding of the associated welfare, fiscal and insurance implications.

## 5. Conclusions

This study provides a step-change in tsunami risk assessment by computing explicitly the possible impact on household welfare.

The process generated 25 earthquake-induced tsunami events, which capture a semi-realistic range of possible future scenarios. It weighed low probability-high impact ones vs. more frequent but less damaging ones by sampling according to a fitted frequency-magnitude law. This pseudo-probabilistic tsunami hazard assessment attempts to represent future tsunamis with a substantial degree of fidelity that forms a basis for the next step of loss modelling. We then used household survey data (STAR1) to understand the impact of tsunamis on household business and non-business assets using the 2004-tsunami experience in Aceh and North Sumatra. Impacts were estimated by regressing changes to asset loss against pre-tsunami household characteristics and intensity dummies. The baseline results showed that households in medium and heavy damaged areas saw an average asset loss of 6% and 33%, respectively, compared to those in no/light loss areas. Assuming externally validity, we then used multinomial logit to fit in Oasis bins for the vulnerability module. The process accounted for the actual spread in losses and a more realistic capture of the impacts of future tsunamis, thus going further than simply using average effects on loss computations.

This novel end-to-end integration of tsunami hazard and economic

consequences may be of substantial interest to Government and agencies in charge of evaluating the potential risk and formulating mitigation policies. For instance, by considering the LEC, the level of capital resource (or insurance) in order to overcome a 200 year event or a 1,000 year event can be determined. The information can also help develop disaster risk insurance products tailored to the local context. These can include Sharia-compliant products, relevant to Islamic finance, as well as microinsurance schemes involving tsunami intensity-related parametric triggers, contributing to lower transaction costs. The use of such products may contribute to sustainable development in countries like Indonesia where private insurance density and penetration is insufficient to mitigate such disasters. The demand for these products can be high especially in areas with a past disaster experience, like in Cilacap, as individuals in such a context tend to be more risk-averse [58].

The use of microeconomic data at the household level also helps to identify losses and damage to micro enterprises, small businesses and household-level assets used to support livelihoods. Thus local governments in particular may be able to identify vulnerabilities faced by these small-holders. For instance, business recovery may be particularly susceptible to disruptions in supply chains. It has been shown, in the context of the Sri Lankan post-2004 tsunami experience, that although there was an influx of aid, business recovery was much slower than commonly assumed, underscoring the role of targeted aid in hastening micro-enterprise recovery [59]. The analysis undertaken by this research can support such targeting by quantifying asset loss at the household level and the subsequent risk by business type, area and other criteria, as relevant. The loss information in the public domain, through educating households and small businesses, may also support disaster preparedness.

Finally, this type of analysis could be utilised in a sector-specific manner, for instance vessels in harbors where fishing is a key part of the livelihood of the local community. Bespoke vulnerability functions of indirect livelihood impacts, due to damage on vessels and nets, could be derived from past surveys allowing specialized risk assessments for harbors.

## Declaration of competing interest

The authors declare that they have no known competing financial interests or personal relationships that could have appeared to influence the work reported in this paper.

## Acknowledgements

\*We acknowledge funding from the Lloyd's Tercentenary Research Foundation, the Lighthill Risk Network and the Lloyd's Register Foundation-Data Centric Engineering Programme of the Alan Turing Institute. We also acknowledge support from the Alan Turing Institute project "Uncertainty Quantification of multi-scale and multiphysics computer models: applications to hazard and climate models" as part of the grant EP/N510129/1 made to the Alan Turing Institute by EPSRC. MH was partly funded by the Royal Society, the United Kingdom, grant number CHL/R1/180173. We thank four anonymous reviewers for their thorough review and insightful comments.

## References

- [1] National Geophysical Data Center/World Data Service: NCEI/WDS Global Historical Tsunami Database. NOAA National Centers for Environmental Information. Accessed in 2020 at URL: [https://www.ngdc.noaa.gov/hazard/tsu\\_db.shtml](https://www.ngdc.noaa.gov/hazard/tsu_db.shtml).
- [2] M. Heidarzadeh, A. Muhari, A.B. Wijanarto, Insights on the source of the 28 september 2018 sulawesi tsunami, Indonesia based on spectral analyses and numerical simulations, *Pure Appl. Geophys.* 176 (1) (2019) 25–43.
- [3] M.C. Frederik, R. Adhitama, N.D. Hananto, S. Sahabuddin, M. Irfan, O. Moefti, D. B. Putra, B.F. Riyalda, et al., First results of a bathymetric survey of palu bay, central sulawesi, Indonesia following the tsunamigenic earthquake of 28 september 2018, *Pure Appl. Geophys.* 176 (8) (2019) 3277–3290.

- [4] M. Heidarzadeh, T. Ishibe, O. Sandanbata, A. Muhari, A.B. Wijanarto, Numerical modeling of the subaerial landslide source of the 22 december 2018 anak Krakatoa volcanic tsunami, Indonesia, *Ocean. Eng.* 195 (2020) 106733.
- [5] A. Paris, P. Heinrich, R. Paris, S. Abadie, The december 22, 2018 anak Krakatau, Indonesia, landslide and tsunami: preliminary modeling results, *Pure Appl. Geophys.* 177 (2) (2020) 571–590.
- [6] K. Goda, N. Mori, T. Yasuda, A. Prasetyo, A. Muhammad, D. Tsujio, Cascading geological hazards and risks of the 2018 Sulawesi Indonesia earthquake and sensitivity analysis of tsunami inundation simulations, *Front. Earth Sci.* 7 (2019) 261.
- [7] A. Muhari, M. Heidarzadeh, H. Susmoro, H.D. Nugroho, E. Kriswati, A. B. Wijanarto, F. Imamura, T. Arikawa, et al., The december 2018 anak Krakatau volcano tsunami as inferred from post-tsunami field surveys and spectral analysis, *Pure Appl. Geophys.* 176 (12) (2019) 5219–5233.
- [8] L. Hamzah, N.T. Puspito, F. Imamura, Tsunami catalog and zones in Indonesia, *J. Nat. Disaster Sci.* 22 (1) (2000) 25–43.
- [9] G. Prasetya, W. De Lange, T. Healy, The Makassar Strait tsunamigenic region, Indonesia, *Nat. Hazards* 24 (3) (2001) 295–307.
- [10] H. M. Fritz, W. Kongko, A. Moore, B. McAdoo, J. Goff, C. Harbitz, B. Uslu, N. Kalligeris, D. Suteja, K. Kalsum, V. Titov, A. Gusman, H. Latief, E. Santoso, S. Sujoko, D. Djulkarnaen, H. Sunendar, C. Synolakis, Extreme runup from the 17 July 2006 Java tsunami, *Geophys. Res. Lett.* 34 (12). doi:10.1029/2007GL029404.
- [11] Y. Fujii, K. Satake, Source of the July 2006 west Java tsunami estimated from tide gauge records, *Geophys. Res. Lett.* 33 (24). doi:10.1029/2006GL028049.
- [12] Y. Tsuji, F. Imamura, H. Matsutomi, C. Synolakis, N. Puspito, Jumadi, S. Harada, S. Han, K. Arai, B. Cook, Field survey of the east Java earthquake and tsunami of June 3, 1994, *Pure Appl. Geophys.* 144 (1995) 839–854, <https://doi.org/10.1007/BF00874397>.
- [13] C. Synolakis, F. Imamura, Y. Tsuji, H. Matsutomi, S. Tinti, B. Cook, Y. Chandra, M. Usman, Damage, conditions of east Java tsunami of 1994 analyzed, *EOS, Trans. Am. Geophys. Union* 76 (26) (1995), 257–257.
- [14] K. Satake, Advances in earthquake and tsunami sciences and disaster risk reduction since the 2004 Indian Ocean tsunami, *Geoscience Letters* 1 (1) (2014) 15.
- [15] A. Gusman, Y. Tanioka, H. Matsumoto, S.-I. Iwasaki, Analysis of the tsunami generated by the great 1977 Sumba earthquake that occurred in Indonesia, *Bulletin of The Seismological Society of America - BULL SEISMOL SOC AMER* 99 (2009) 2169–2179, <https://doi.org/10.1785/0120080324>.
- [16] E.A. Okal, The south of Java earthquake of 1921 September 11: a negative search for a large interplate thrust event at the Java Trench, *Geophys. J. Int.* 190 (3) (2012) 1657–1672, <https://doi.org/10.1111/j.1365-246X.2012.05570.x>.
- [17] G. Ram, L. McGuinness, Microinsurance Demand and Market Prospects: Indonesia (2005).
- [18] SwissRe, Regional details and data appendix, world insurance: regional review 2019, and outlook, *Sigma* 4/2020 (2020) 1–20.
- [19] T. Baba, N. Takahashi, Y. Kaneda, K. Ando, D. Matsuoka, T. Kato, Parallel implementation of dispersive tsunami wave modeling with a nesting algorithm for the 2011 Tohoku tsunami, *Pure Appl. Geophys.* 172 (12) (2015) 3455–3472, <https://doi.org/10.1007/s00024-015-1049-2>.
- [20] T. Baba, K. Ando, D. Matsuoka, M. Hyodo, T. Hori, N. Takahashi, R. Obayashi, Y. Imato, D. Kitamura, H. Uehara, T. Kato, R. Saka, Large-scale, high-speed tsunami prediction for the great Nankai trough earthquake on the K computer, *Int. J. High Perform. Comput. Appl.* 30 (1) (2016) 71–84, <https://doi.org/10.1177/1094342015584090>.
- [21] K. Satake, M. Heidarzadeh, A review of source models of the 2015 Illapel, Chile earthquake and insights from tsunami data, *Pure Appl. Geophys.* 174 (1) (2017) 1–9.
- [22] T. Baba, Y. Gon, K. Imai, K. Yamashita, T. Matsuno, M. Hayashi, H. Ichihara, Modeling of a dispersive tsunami caused by a submarine landslide based on detailed bathymetry of the continental slope in the Nankai Trough, southwest Japan, *Tectonophysics* 768 (2019) 228182, <https://doi.org/10.1016/j.tecto.2019.228182>.
- [23] D.M. Salmanidou, M. Heidarzadeh, S. Guillas, Probabilistic landslide-generated tsunamis in the Indus canyon, NW Indian ocean, using statistical emulation, *Pure Appl. Geophys.* 176 (7) (2019) 3099–3114, <https://doi.org/10.1007/s00024-019-02187-3>.
- [24] Y. Okada, Surface deformation due to shear and tensile faults in a half-space, *Bull. Seismol. Soc. Am.* 75 (4) (1985) 1135–1154.
- [25] C. J. Ammon, H. Kanamori, T. Lay, A. A. Velasco, The 17 July 2006 Java tsunami earthquake, *Geophys. Res. Lett.* 33 (24). doi:<https://doi.org/10.1029/2006GL028005>.
- [26] H. Hébert, P.-E. Burg, R. Binet, F. Lavigne, S. Allgeyer, F. Schindelé, The 2006 July 17 Java (Indonesia) tsunami from satellite imagery and numerical modelling: a single or complex source?: 2006 Java tsunami: earthquake or landslide? *Geophys. J. Int.* (2012) 1255, <https://doi.org/10.1111/j.1365-246X.2012.05666.x>.
- [27] R. McCaffrey, The next great earthquake, *Science* 315 (5819) (2007) 1675–1676.
- [28] S. Stein, E.A. Okal, Ultralong period seismic study of the December 2004 Indian Ocean earthquake and implications for regional tectonics and the subduction process, *Bull. Seismol. Soc. Am.* 97 (1A) (2007) S279–S295.
- [29] K. Satake, M. Heidarzadeh, M. Quiroz, R. Cienfuegos, History and features of trans-oceanic tsunamis and implications for paleo-tsunami studies, *Earth Sci. Rev.* (2020) 103112.
- [30] M. Heidarzadeh, M.D. Pirooz, N.H. Zaker, Modeling the near-field effects of the worst-case tsunami in the Makran subduction zone, *Ocean. Eng.* 36 (5) (2009) 368–376.
- [31] K. Satake, K. Shimazaki, Y. Tsuji, K. Ueda, Time and size of a giant earthquake in Cascadia inferred from Japanese tsunami records of January 1700, *Nature* 379 (6562) (1996) 246–249.
- [32] K. Jankaew, B.F. Atwater, Y. Sawai, M. Choowong, T. Charoentitirat, M.E. Martin, A. Prendergast, Medieval forewarning of the 2004 Indian Ocean tsunami in Thailand, *Nature* 455 (7217) (2008) 1228–1231.
- [33] N. Horspool, I. Pranantyo, J. Griffin, H. Latief, D. Natawidjaja, W. Kongko, A. Cipta, B. Bustaman, S. Anugrah, H. Thio, A probabilistic tsunami hazard assessment for Indonesia, *Nat. Hazards Earth Syst. Sci.* 14 (11) (2014) 3105–3122.
- [34] E.L. Geist, T. Parsons, Probabilistic analysis of tsunami hazards, *Nat. Hazards* 37 (3) (2006) 277–314.
- [35] D.L. Wells, K.J. Coppersmith, New empirical relationships among magnitude, rupture length, rupture width, rupture area, and surface displacement, *Bull. Seismol. Soc. Am.* 84 (4) (1994) 974–1002.
- [36] E. Frankenberg, P. Katz, I.U. Rifai, B. Sikoki, C. Sumantri, W. Surtastini, T. Duncan, Study of the tsunami aftermath and recovery (STAR): study design and results, Project Report (2020) 29.
- [37] E. Frankenberg, T. Gillespie, S. Preston, B. Sikoki, D. Thomas, Mortality, the family and the Indian Ocean tsunami, *Econ. J.* 121 (554) (2011) F162–F182.
- [38] A.G. Cas, E. Frankenberg, W. Surtastini, D. Thomas, The impact of parental death on child well-being: evidence from the Indian Ocean tsunami, *Demography* 51 (2) (2014) 437–457.
- [39] Y. Sawada, Y. Takasaki, Natural disaster, poverty, and development: an introduction, *World Dev.* 94 (2017) 2–15.
- [40] E. Skoufias, Economic crises and natural disasters: coping strategies and policy implications, *World Dev.* 31 (7) (2003) 1087–1102.
- [41] T. Deryugina, L. Kawano, S. Levitt, The economic impact of hurricane Katrina on its victims: evidence from individual tax returns, *Am. Econ. J. Appl. Econ.* 10 (2) (2018) 202–233.
- [42] M. Kirchberger, Natural disasters and labor markets, *J. Dev. Econ.* 125 (2017) 40–58.
- [43] J.D. Kang, J.L. Schafer, et al., Demystifying double robustness: a comparison of alternative strategies for estimating a population mean from incomplete data, *Stat. Sci.* 22 (4) (2007) 523–539.
- [44] P.R. Rosenbaum, D.B. Rubin, The central role of the propensity score in observational studies for causal effects, *Biometrika* 70 (1) (1983) 41–55.
- [45] J. Antilla-Hughes, M. Sharma, Linking Risk Models to Microeconomic Indicators, The World Bank, 2015.
- [46] A. Abadie, G.W. Imbens, Large sample properties of matching estimators for average treatment effects, *Econometrica* 74 (1) (2006) 235–267.
- [47] G.W. Imbens, J.M. Wooldridge, Recent developments in the econometrics of program evaluation, *J. Econ. Lit.* 47 (1) (2009) 5–86.
- [48] M.D. Cattaneo, Efficient semiparametric estimation of multi-valued treatment effects under ignorability, *J. Econom.* 155 (2) (2010) 138–154.
- [49] J. M. Wooldridge, *Econometric Analysis of Cross Section and Panel Data*, MIT press, 2010.
- [50] J. Strauss, F. Witoelar, B. Sikoki, The Fifth Wave of the Indonesia Family Life Survey: Overview and Field Report: Volume vol. 1.
- [51] J. Sanyal, X.X. Lu, Application of remote sensing in flood management with special reference to monsoon Asia: a review, *Nat. Hazards* 33 (2) (2004) 283–301.
- [52] R. Himaz, H. Aturupane, Why are boys falling behind? Explaining gender gaps in school attainment in Sri Lanka, *World Dev.* 142 (June) (2021) 105415.
- [53] B. Gutenberg, C.F. Richter, Frequency of earthquakes in California\*, *Bull. Seismol. Soc. Am.* 34 (4) (1944) 185–188.
- [54] C.M. Rubin, B.P. Horton, K. Sieh, J.E. Pilarczyk, P. Daly, N. Ismail, A.C. Parnell, Highly variable recurrence of tsunamis in the 7,400 years before the 2004 Indian Ocean tsunami, *Nat. Commun.* 8 (2017) 16019.
- [55] D. Salmanidou, S. Guillas, A. Georgiopolou, F. Dias, Statistical emulation of landslide-induced tsunamis at the rockall bank, NE Atlantic, *Proc. Math. Phys. Eng. Sci.* 473 (2200) (2017) 20170026.
- [56] S. Guillas, A. Sarri, S.J. Day, X. Liu, F. Dias, et al., Functional emulation of high resolution tsunami modelling over Cascadia, *Ann. Appl. Stat.* 12 (4) (2018) 2023–2053.
- [57] D. Gopinathan, M. Heidarzadeh, S. Guillas, Probabilistic quantification of tsunami currents in Karachi port, Makran subduction zone, using statistical emulation, *Earth and Space Science Open Archive* (2020) 38doi, <https://doi.org/10.1002/essoar.10502534.2>.
- [58] L. Cameron, M. Shah, Risk-taking behavior in the wake of natural disasters, *J. Hum. Resour.* 50 (2) (2015) 484–515.
- [59] S. De Mel, D. McKenzie, C. Woodruff, Enterprise recovery following natural disasters, *Econ. J.* 122 (559) (2012) 64–91.